

Isomerism in Supramolecular Adducts of Atomically Precise Nanoparticles

Abhijit Nag, Papri Chakraborty, Ganesan Paramasivam, Mohammad Bodiuzzaman, Ganapati Natarajan, and Thalappil Pradeep*[✉]

DST Unit of Nanoscience and Thematic Unit of Excellence, Department of Chemistry, Indian Institute of Technology Madras, Chennai-600036, India

Supporting Information

ABSTRACT: We present isomerism in a few supramolecular adducts of atomically precise nanoparticles, $[\text{Ag}_{29}(\text{BDT})_{12} \cap (\text{CD})_n]^{3-}$ ($n = 1-6$), abbreviated as **I** where BDT and CD are 1,3-benzenedithiol and cyclodextrins (α , β and γ), respectively; \cap symbolizes an inclusion complex. The different host–guest complexes of **I** were characterized in the solution state as well as in the gas phase. The CDs (α , β and γ) encapsulate a pair of BDT ligands protecting the Ag_{29} core. This unique geometry of the supramolecular adducts makes the system similar to octahedral complexes of transition metals, which manifest various isomers. These isomers of **I** ($n = 2-4$) were separated by ion mobility mass spectrometry (IM MS). We proposed structures of all the inclusion complexes with the help of IM MS measurements and molecular docking, density functional theory (DFT), and collision cross section (CCS) calculations.

Atomically precise nanoparticles of noble metals with precise composition and structure exhibiting characteristic properties^{1–4} are an important class of molecules showing potential applications in energy conversion,⁵ sensing,⁶ catalysis^{7,8} and biomedical applications.⁹ Their molecular science is gradually evolving, an important aspect being intercluster reactions.^{10–13} Supramolecular chemistry is playing a key role in intercluster interactions to assemble clusters through weak interactions between ligands arising from directed hydrogen-bonding,¹⁴ electrostatic, and C–H $\cdots\pi$ interactions.¹⁵ One of the characteristics of molecular systems is isomerism, which has been important in the evolution of science, especially that of transition metal coordination complexes. Theoretical and experimental efforts to find structural isomerism in nanoclusters^{16,17} will provide new insights into designing unique functional materials.

The shape-sensitive hydrophobic cavities of CDs represent a class of receptors that are ideal for the construction of hybrid assemblies.^{18,19} The formation of supramolecular adducts of $\text{Au}_{25}(\text{SBB})_{18}$, where SBB is 4-(*t*-butyl)benzyl mercaptan, with CD was reported previously.²⁰

Here, we establish the occurrence of isomerism in CD adducts of an atomically precise nanoparticle. First, we created supramolecular adducts of $[\text{Ag}_{29}(\text{BDT})_{12}]^{3-}$ (BDT = 1, 3 benzenedithiol) abbreviated as X^{3-} , with CDs. They are labeled as $\text{X} \cap (\text{CD})_n^{3-}$; the symbolism, $\text{A} \cap \text{B}$ represents an

inclusion complex of **A** in **B**.²¹ Isomers were detected for $n = 2, 3$ and 4 complexes by IM MS, while $n = 1, 5$ and 6 adducts did not show isomers, as in octahedral complexes. The experimental observations were fully supported by molecular docking, DFT, and CCS calculations.

We prepared $\text{X} \cap (\text{CD})_{1-6}^{3-}$ clusters in dimethylformamide by careful mixing of X^{22} and CDs (α , β and γ) in various proportions and their electrospray ionization mass spectrometry (ESI MS) were performed, as shown in Supporting Information (Figures S2–S6). The cluster, X^{3-} , was synthesized following the reported protocol²² with slight modifications as described in the Experimental Details (Supporting Information) and characterized using optical absorption and ESI MS (Figure S1). The spectrum of 1:6 mixture of X^{3-} with β -CD is shown in Figure 1, which exhibited $n = 1-6$ β -CD adducts of the cluster in substantial intensity. Each of these adducts exhibited well-resolved mass spectra showing all the

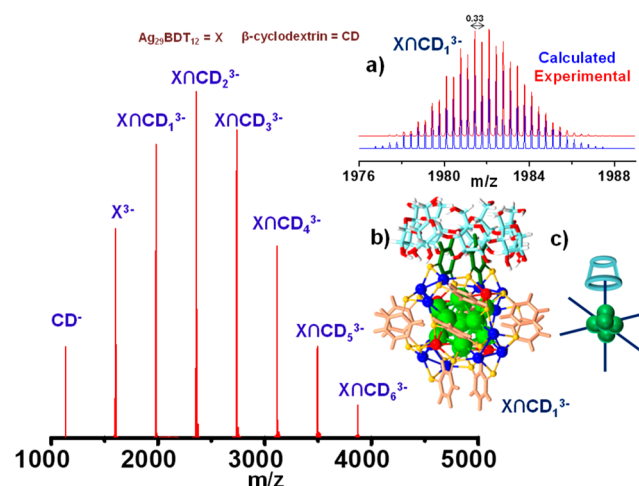


Figure 1. ESI MS of $[\text{X} \cap (\text{CD})_n]^{3-}$ ($n = 1$ to 6) (**I**) supramolecular complexes, where **X** and **CD** represent $\text{Ag}_{29}(\text{BDT})_{12}$ and β -cyclodextrin. (a) Theoretical and experimental isotopic patterns for $[\text{X} \cap (\text{CD})_n]^{3-}$. (b) Schematic representation of **I** for $n = 1$. Color codes: Ag_{13} Core, light green; 4 Ag_3 staples, blue; 4 Ag tetrahedral positions, red; sulfur, yellow; carbon, brown. Encapsulated BDTs in CD are in dark green. (c) A simple representation of **I** for $n = 1$, similar to an octahedral coordination geometry.

Received: August 23, 2018

Published: October 10, 2018

expected isotopologues (Figure 1a). This, along with the fragmentation patterns, confirmed their composition. The adducts lost CD upon collisional activation (Figures S7–S10). Energy threshold needed for the loss increases with the increase in diameter of CDs from α to γ , suggesting increased interactions with increasing diameter of the cavity (Figure S11). From a comparison of the absorption spectra of the adducts with that of the cluster, it appeared that the absorption features of the adducts were mainly additive with slight changes^{19,23} in the absorbances of the constituents indicating that electronic structure of the cluster is almost unaffected by CD complexation (Figure S12). Upon addition of β -CD in X^{3-} in DMF- D_7 (Figure S13), 1H NMR spectra showed significant changes in the resonances for the H-1, H-3 and H-5 protons.¹⁹ The changing signals of H-1, H-3 and H-5 suggest that the ligands are deeply inserted in the CD cavity.¹⁹ The observation of a maximum of six CD adducts in ESI MS and the NMR results indicated that probably each CD encapsulates a pair of BDT ligands on the cluster surface. Previous study of supramolecular functionalization of $Au_{25}SBB_{18}^-$ with β -CD showed that each CD encapsulated only one SBB ligand due to their radially outward orientation which were spaced farther apart.²⁰ We will come back to this aspect when we discuss the computational data.

The attachment of six CDs could imply an octahedral arrangement of CDs on the cluster surface that can result in structural isomers as seen in coordination complexes. If two ligands in an octahedral complex are different from the other four, giving an MA_4B_2 complex, two isomers are possible. The two B ligands can be *cis* or *trans* as shown in Figure S14B. Replacing another A ligand by B gives an MA_3B_3 complex for which there are also two possible isomers. In one, the three ligands of each kind occupy opposite triangular faces of the octahedron; this is called the “*fac*” isomer (for facial) (Figure S14C). In the other, when three ligands are found in a row of an octahedron, it is called “*mer*” isomer (for meridional) (Figure S14C). In contrast, such isomerism is impossible in tetrahedral systems as all the sites are equivalent.

In this discussion, the free and CD included BDTs can be considered as two different ligands, A and B, respectively. For example, $X\cap CD_2$ can be considered as MA_4B_2 where M corresponds to Ag_{29} , A corresponds to BDT_2 as the two BDT ligands get included in one CD and B corresponds to $BDT_2\cap CD$.

IM MS can effectively separate structural isomers in the gas phase. The drift time profile of various supramolecular adducts shown in Figure 2 reveals the existence of isomers in some of the β -CD adducts. While the adducts for $n = 1, 5$ and 6 do not reveal isomers, the other adducts, $n = 2–4$ show two distinct isomers with differing populations. These resemble the situation encountered in octahedral coordination complexes. The mass spectra extracted from the drift time profiles reveal the isomeric nature of the species (Figures S15–S17). The experimental CCS value for each complex is given in Figure 2. It further shows the increasing difference in the CCS with increasing the number of β -CDs. The $X\cap(\beta-CD)_5$ (Figure 2e) peak is only 13% broader than $X\cap(\beta-CD)_1$ and $X\cap(\beta-CD)_6$ peaks (Figure 2a,d). So, there are fewer possibilities to have multiple isomers. In the case of other CD functionalized clusters like $Au_{25}SBB_{18}\cap CD_n$ ($n = 2, 3$ and 4), there may be some possibilities for isomerism.

In order to understand the structures of the complexes, we performed molecular docking²⁴ and DFT calculations. To

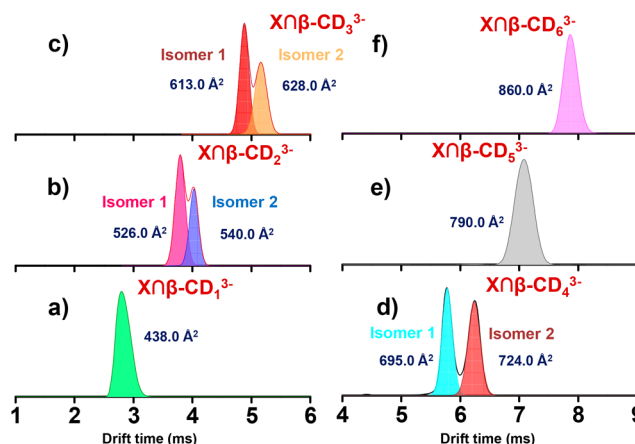


Figure 2. (a–f) Drift time profile of $[X\cap(\beta-CD)_n]^{3-}$ ($n = 1$ to 6) complexes and their corresponding CCS values. (b, c and d) Presence of isomers in the complexes when $n = 2, 3$ and 4.

verify the lowest energy structure of $X\cap CD$, we carried out a global structure search by molecular docking simulations using minimum energy geometry of the adduct. More details about docking and DFT calculations are provided in the computational section of SI. Docking study shows that a pair of BDT ligands gets into the cavity of CDs (Figure S18). The lowest energy docked structures of $X\cap CD$ (α , β and γ) were used for DFT optimization. The binding energy (BE) values in PBE (Perdew, Burke and Ernzerhof) method for $X\cap\alpha$ -CD, $X\cap\beta$ -CD and $X\cap\gamma$ -CD were -33.46 , -65.15 and -69.01 kcal/mol, respectively (Figure 3). With increase of diameter of the CD,

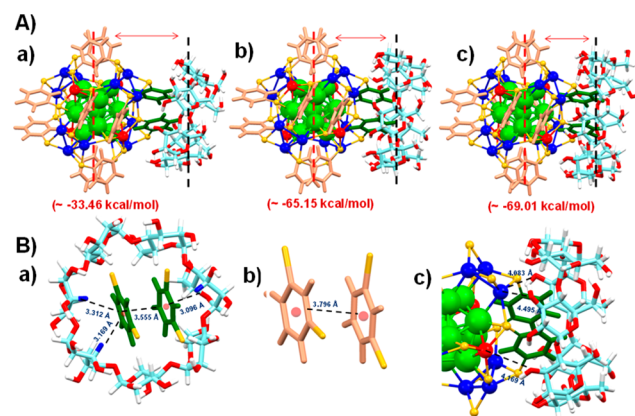


Figure 3. (Aa–c) DFT optimized lowest energy structures of $[X\cap(CD)_n]^{3-}$ complexes where CD stands for α , β and γ -CD, respectively. The distance between the CD and the cluster decreases with increasing diameter of the CD. (Ba) The C–H... π interactions between BDTs and β -CD. (Bb) The π – π interaction distance between two BDTs. (Cc) The Ag...O interaction distances with β -CD.

the BE of the adducts is increasing which is in good agreement with the CID experiment shown in Figure S11. As the cavity size increases, a pair of BDT ligands can penetrate more inside the cavity. Here, C–H... π , weak ionic $Ag\cdots O$, hydrogen bonding and van der Waals (vdWs) interactions are the main reasons for such complexation. For β -CD, the C–H... π interaction distances were ~ 3.09 to 3.31 Å. The distance between the two BDT ligands decreases when CD encapsulated them (Figure 3Ba,b), which enhances the π – π interactions between the BDT ligands in the complex. For β -

CD, the Ag...O interaction distances were ~ 4.08 to 4.49 Å. The Ag...O interaction increases from α to γ CD. Furthermore, Ag–S distance involving core Ag atoms was elongated by 0.04 Å whereas the Ag–S distance of the staple was reduced by 0.06 Å. Hydrogen bonding interactions are also expected to play a key role in the complexation of a β -CD ligand with X. It is worth noting that the ionic interaction between multiple S atoms on the cluster and H of CD ligand mainly influences the interaction of β -CD with the X cluster. Particularly, the strong ionic interaction of S...H shows a distance of 2.11 – 2.80 Å. On the other hand, hydrogen bonding distances 3.37 – 3.86 Å are found between O of the CD and nearest H of the BDT ligands. To study the effect of vdW interactions, the structures were again reoptimized using a vdW-DF2/DZP methodology and the resulting BEs were compared with those of PBE/DZP methodology (Table S1). We have checked the other encapsulation possibility of CDs from the tail side (Figure S19) also. But in this case, the complex is less stable.

These structures can be drawn in a simpler fashion as shown in Figure 4. We see that the ligand orientation in X^{3-} displays

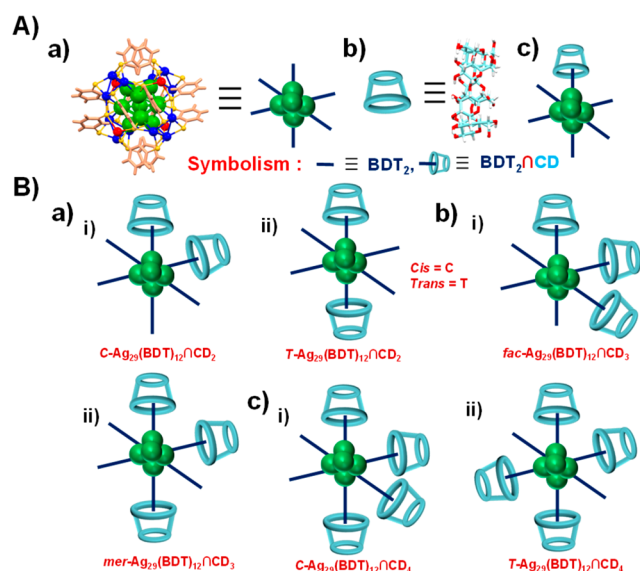


Figure 4. (Aa–c) Schematic representation of X, CD and $[Xn(CD)n]^{3-}$, respectively. (Ba–c) Simple representation of C/T isomers of $[Xn(CD)n]^{3-}$ $n = 2$ and 4 , respectively. (Bb) The *fac-mer* isomers of $[Xn(CD)n]^{3-}$ ($n = 3$).

an octahedral symmetry, if we consider a pair of BDT as one unit (Figure 4Aa). This simple diagram illustrates the similarity of such complexes with octahedral coordination complexes. At the same time, it confirms the distinct structural possibilities in supramolecular adducts derived from the cluster. The adduct, $[Xn(CD)n]^{3-}$ has only one structural isomer as all ligand units are identical (Figure 4Ac) while $[Xn(CD)_2]^{3-}$ will have two possible isomers, *cis* (C) and *trans* (T) (Figure 4Ba). There are similar possibilities in $[Xn(CD)_3]^{3-}$, which can also exhibit *fac-mer* isomerism (Figure 4Bb). Such an analysis presents two isomers for $[Xn(CD)_4]^{3-}$ also (Figure 4Bc). $[Xn(CD)_6]^{3-}$ represents an octahedral symmetry by covering the whole cluster with CDs with no isomers (Figure S21). Same is the case with $[Xn(CD)_5]^{3-}$ also. The IM MS results agree with this (Figure 2).

For $[Xn\beta\text{-CD}_n]^{3-}$ ($n > 1$) complexes were optimized by using the PBE²⁵ and vdW-DF2 functionals. PBE functional

results and BEs are presented in Figure S20. The *cis* isomers are more stable compared to the *trans* isomer because of extra hydrogen bonding between the CDs. The DFT optimized structures were further used to calculate the CCSs. The calculated CCSs are in agreement with the experimental CCSs obtained from IM MS allowing accurate assignment (Table S2). The relative populations of the adducts ($n = 2$ – 4) observed in the mobilogram can be correlated with the stabilization energy as shown in Figure S20. The calculated and experimental CCS values are given in Table S2. DFT optimized structures of $[Xn\beta\text{-CD}_n]^{3-}$ for $n = 5$ and 6 are given in Figure S21. Now, it is possible to assign isomers 1 and 2 of Figure 2b and d as *cis* and *trans*, respectively. The isomer 1 and isomer 2 of Figure 2c represent the *fac* and *mer* isomers, respectively.

Concerning the implication of the structures, we propose that their isolation in the solid state can result in new kinds of cluster-assembled materials. Supramolecular complexation in such systems may introduce new properties like chirality. Although these are speculative at the moment, we postulate that such supramolecular complexes discussed here may introduce new aspects in the science of atomically precise clusters.

In summary, we synthesized supramolecular complexes of atomically precise clusters with CDs. We proposed isomeric structures of such supramolecular complexes which are reminiscent of coordination complexes. These isomers were separated using IM MS. The obtained CCSs from the experiments were compared with those of the calculated structures. The agreement between the theory and experiment in CCSs and relative populations support the proposed structures. Supramolecular isomerism could be observed for other clusters also depending on the symmetry, orientation and geometry of the ligand surrounding the cluster. We postulate that the discovery of new clusters with amenable ligands would enhance better stabilization of such complexes, allowing the isomers to be used as precursors for new cluster-based materials.

■ ASSOCIATED CONTENT

§ Supporting Information

The Supporting Information is available free of charge on the ACS Publications website at DOI: 10.1021/jacs.8b08767.

Experimental details, computational details, ESI MS, NMR results, DFT optimized structures, molecular docking study and CCS calculations (PDF)

Computational data (PDF)

■ AUTHOR INFORMATION

Corresponding Author

*pradeep@iitm.ac.in

ORCID

Thalappil Pradeep: 0000-0003-3174-534X

Notes

The authors declare no competing financial interest.

■ ACKNOWLEDGMENTS

We thank the Department of Science and Technology, Government of India for constantly supporting our research program on nanomaterials. A.N. thanks IIT Madras for a doctoral fellowship. P.C. thanks the Council of Scientific and

Industrial Research (CSIR) for her research fellowship. M.B. thanks the University Grants Commission (UGC) for his research fellowship. G.P. thanks IIT Madras for an Institute Postdoctoral fellowship.

■ REFERENCES

- (1) Parker, J. F.; Fields-Zinna, C. A.; Murray, R. W. *Acc. Chem. Res.* **2010**, *43*, 1289–1296.
- (2) Maity, P.; Xie, S.; Yamauchi, M.; Tsukuda, T. *Nanoscale* **2012**, *4*, 4027–4037.
- (3) Jin, R.; Zeng, C.; Zhou, M.; Chen, Y. *Chem. Rev.* **2016**, *116*, 10346–10413.
- (4) Chakraborty, I.; Pradeep, T. *Chem. Rev.* **2017**, *117*, 8208–8271.
- (5) Mathew, A.; Pradeep, T. *Part. Part. Syst. Char.* **2014**, *31*, 1017–1053.
- (6) Yuan, X.; Luo, Z.; Yu, Y.; Yao, Q.; Xie, J. *Chem. - Asian J.* **2013**, *8*, 858–871.
- (7) Yamazoe, S.; Koyasu, K.; Tsukuda, T. *Acc. Chem. Res.* **2014**, *47*, 816–824.
- (8) Kurashige, W.; Niihori, Y.; Sharma, S.; Negishi, Y. *Coord. Chem. Rev.* **2016**, 320–321, 238–250.
- (9) Song, X.-R.; Goswami, N.; Yang, H.-H.; Xie, J. *Analyst* **2016**, *141*, 3126–3140.
- (10) Krishnadas, K. R.; Baksi, A.; Ghosh, A.; Natarajan, G.; Pradeep, T. *Nat. Commun.* **2016**, *7*, 13447.
- (11) Krishnadas, K. R.; Ghosh, A.; Baksi, A.; Chakraborty, I.; Natarajan, G.; Pradeep, T. *J. Am. Chem. Soc.* **2016**, *138*, 140–148.
- (12) Krishnadas, K. R.; Baksi, A.; Ghosh, A.; Natarajan, G.; Pradeep, T. *ACS Nano* **2017**, *11*, 6015–6023.
- (13) Krishnadas, K. R.; Baksi, A.; Ghosh, A.; Natarajan, G.; Som, A.; Pradeep, T. *Acc. Chem. Res.* **2017**, *50*, 1988–1996.
- (14) Chakraborty, A.; Fernandez, A. C.; Som, A.; Mondal, B.; Natarajan, G.; Paramasivam, G.; Lahtinen, T.; Häkkinen, H.; Nonappa; Pradeep, T. *Angew. Chem., Int. Ed.* **2018**, *57*, 6522–6526.
- (15) Nag, A.; Chakraborty, P.; Bodiuzzaman, M.; Ahuja, T.; Antharjanam, S.; Pradeep, T. *Nanoscale* **2018**, *10*, 9851–9855.
- (16) Tian, S.; Li, Y.-Z.; Li, M.-B.; Yuan, J.; Yang, J.; Wu, Z.; Jin, R. *Nat. Commun.* **2015**, *6*, 8667.
- (17) Chen, Y.; Liu, C.; Tang, Q.; Zeng, C.; Higaki, T.; Das, A.; Jiang, D.-e.; Rosi, N. L.; Jin, R. *J. Am. Chem. Soc.* **2016**, *138*, 1482–1485.
- (18) Wu, Y.; Shi, R.; Wu, Y.-L.; Holcroft, J. M.; Liu, Z.; Frascioni, M.; Wasielewski, M. R.; Li, H.; Stoddart, J. F. *J. Am. Chem. Soc.* **2015**, *137*, 4111–4118.
- (19) Moussawi, M. A.; Leclerc-Laronze, N.; Floquet, S.; Abramov, P. A.; Sokolov, M. N.; Cordier, S.; Ponchel, A.; Monflier, E.; Bricout, H.; Landy, D.; Haouas, M.; Marrot, J.; Cadot, E. *J. Am. Chem. Soc.* **2017**, *139*, 12793–12803.
- (20) Mathew, A.; Natarajan, G.; Lehtovaara, L.; Häkkinen, H.; Kumar, R. M.; Subramanian, V.; Jaleel, A.; Pradeep, T. *ACS Nano* **2014**, *8*, 139–152.
- (21) Lehn, J.-M. *From Molecular to Supramolecular Chemistry. Supramolecular Chemistry*; Wiley-VCH Verlag GmbH & Co. KGaA: 2006; pp 1–9.
- (22) AbdulHalim, L. G.; Bootharaju, M. S.; Tang, Q.; Del Gobbo, S.; AbdulHalim, R. G.; Eddaoudi, M.; Jiang, D.-e.; Bakr, O. M. *J. Am. Chem. Soc.* **2015**, *137*, 11970–11975.
- (23) Chakraborty, P.; Nag, A.; Paramasivam, G.; Natarajan, G.; Pradeep, T. *ACS Nano* **2018**, *12*, 2415–2425.
- (24) Morris, G. M.; Huey, R.; Lindstrom, W.; Sanner, M. F.; Belew, R. K.; Goodsell, D. S.; Olson, A. J. *J. Comput. Chem.* **2009**, *30*, 2785–2791.
- (25) Perdew, J. P.; Burke, K.; Ernzerhof, M. *Phys. Rev. Lett.* **1997**, *78*, 1396–1396.